Submitted on February 2013. Revised on May 10, 2013 and on June 22, 2013. Accepted on June 26, 2013.

Measurement and Characterization of Load Impedances in Home Power Line Grids

Massimo Antoniali and Andrea M. Tonello, *Senior Member*, *IEEE*

Department of Electrical Mechanical and Management Engineering, Università di Udine
Via delle Scienze 208, 33100 Udine, Italy
massimo.antoniali@uniud.it, tonello@uniud.it

***Abstract*—The measurement and characterization of the load impedances in the home/office power grid is the topic of this paper. This is motivated by the interest of exploiting the home power line grid for data communications. The power line communication (PLC) medium is strongly affected by the presence of unmatched and time variant loads so that we have carried out a measurement campaign on a representative set of devices that can be found in a house or office. The measurement procedure has allowed the investigation of their behavior both in the time and in the frequency domain, over a time span equal to the mains period and within the frequency range 2-30 MHz that is used by broad band PLC systems. We have found a very limited number of devices with an impedance noticeably time variant. This is because they include, in the power supply unit, an electromagnetic interference (EMI) filter that significantly reduces the time variant behavior of the device impedance in the 2-30 MHz band. Furthermore, the impedance of any device is also affected by the presence of a power cord. Finally, from the experimental results, we propose a behavioral classification of the devices based on certain typical time/frequency characteristics of their impedance.**

***Index Terms*— Load impedance, Power line communication (PLC), Power supply, Electromagnetic interference filter, Home grid communication systems, Load measurements.**

Submitted on February 2013. Revised on May 10, 2013 and on June 22, 2013. Accepted on June 26, 2013.

I. INTRODUCTION

POWER line communication (PLC) exploits the existing power grid to convey data signals. There are several application scenarios of PLC, such as the smart grid and the home networking scenarios [1]. However, since the power grid has not been designed for data communications, the transmission medium is hostile and exhibits high attenuation, multipath propagation and frequency selectivity, due to the presence of branches, discontinuities and unmatched loads.

Some early work on modeling the characteristics of the in-home power line transmission medium at high frequencies (up to 30 MHz) has been done in [2]-[4]. It has been recognized that the PLC channel response is affected by the presence of transformers [5] and electrical device (load) impedances [6]-[9]. The knowledge of the load impedances allows the prediction of the channel transfer function through the application of a bottom-up channel modeling approach that uses transmission line theory applied to a certain network topology, as it is done, for instance, in [10]-[12]. This approach computes the channel transfer function when the wire topology, the wire electrical characteristics, and the load impedances are known. Furthermore, the electrical devices connected to the power grid are the main sources of noise in the in-home PLC as discussed in [13]-[14].

In this paper, we describe a measurement procedure for the characterization of the impedance (in the high frequency range 2-30 MHz) of devices encountered in home PLC networks. The procedure has been applied to characterize a set of devices that can be found in a typical house or office, i.e., home appliances, office equipment and lighting system components. The devices have been collected in Italy where the mains signal has amplitude 230 V (r.m.s.) and frequency 50 Hz. The purpose is to analyze the time/frequency impedance characteristics of such devices in order to enable the prediction of their impact on the overall channel response in typical PLC home networks.

The measurement procedure works in the frequency domain using a vector network analyzer (VNA). Other methodologies to measure time variant loads have been reported in [15], [16].

Submitted on February 2013. Revised on May 10, 2013 and on June 22, 2013. Accepted on June 26, 2013.

The procedure allows the study of the behavior in the time and in the frequency domain of the loads in terms of the voltage-to-current relation between the two feeding conductors, i.e., the line (hot) and the neutral wires. In most of the devices, the relation between voltage and current is linear and time invariant, i.e., the devices can be modeled as linear time invariant (LTI) loads characterized by their own frequency dependent impedances $Z(f)$. However, there exist some devices whose behavior is not linear and varies with time according to the sinusoidal mains signal. The loads time variant behavior is responsible of the time variant behavior of the PLC channel response. In [9], these devices are modeled as linear periodic time variant (LPTV) loads characterized by a time variant impedance $Z(t,f)$ that changes periodically and synchronously with the mains cycle. As a consequence, the presence of time variant loads causes the channel response to be periodically time variant. Two classes of LPTV devices have been identified. The first group of devices is characterized by two distinct states of impedance that vary within the mains cycle with a repetition rate of 100 Hz. The devices of the second group are instead characterized by less pronounced variations between the two states of impedance with a repetition rate of 50 Hz.

We have investigated the time variant behavior of the devices digging into the cause of it. Our measurement procedure has shown that what causes the time variant behavior of these devices is the uncontrolled rectifier of the front-end circuitry of their power supply unit. Interestingly, in our campaign we have found that most of the devices are actually time invariant. This is because they are equipped with an electromagnetic interference (EMI) filter to fulfill electromagnetic compatibility norms [17], [18]. We will show that the EMI filter significantly reduces the time variant behavior of the load. Furthermore, most of the devices that we can find in a house or office are equipped with a power cord which has a dominant effect on the overall impedance profile. Consequently, in networks with such loads the channel response will result mainly time invariant.

Finally, based on the measurement results, we propose a classification of the devices according to their time/frequency impedance characteristics.

Submitted on February 2013. Revised on May 10, 2013 and on June 22, 2013. Accepted on June 26, 2013.

This paper is organized as follows. In Section II, we analyze the characteristics of the impedance of the electrical devices. Sections III and IV investigate the effect of the aforementioned EMI filter and power cord on the behavior of the load impedance. In Section V, we propose a classification of the measured devices. Finally, the conclusions follow.

II. Measurement procedure and Analysis of the Load Impedance Behavior

In general, typical electrical devices that we can find in a house or office can be divided in two groups. Devices that are substantially ohmic loads, e.g., a toaster or a steam iron, and devices with a more complex behavior because they deploy a power supply unit. Usually, the devices are equipped with an electrical plug and with a power cord. The power cord is sometimes omitted, e.g., in the case of mobile phone chargers. The power supply unit is often equipped with noise suppression capacitors or more complex electromagnetic interference (EMI) filters. In the following, we describe a measurement procedure that has been used to characterize the impedance of a broad set of devices (specifically: a number of PC power supplies, mobile phone chargers, halogen lamps with electronic ballasts, a compact fluorescent lamp, a desk lamp, a vacuum cleaner, a coffee machine, a refrigerator, a microwave oven, an electrical steam cooker, a cooking mixer, an hairdryer, a DVD player, a CD player, an audio amplifier and a drill).

The measurements have been performed in the frequency domain using a vector network analyzer (VNA). We measured the reflection coefficient of the device under test (DUT) from which the impedance value was obtained. Fig. 1 depicts the schematic of the load impedance measurement setup and the block diagram of the input stage of typical electrical devices. We exploited the zero-span mode of the VNA, which enables the evaluation of the reflection coefficient at a certain frequency in a finite number of time instants. We fixed the time span equal to the mains period, i.e., 20 ms, thus we investigated the time variant behavior of the DUTs assuming the loads to be periodically time variant with a repetition frequency integer multiple of the mains frequency. The acquisition was triggered on the 50 Hz mains signal and was done in the frequency band 2-30 MHz. A capacitive coupler was used to protect the equipment from the mains

Submitted on February 2013. Revised on May 10, 2013 and on June 22, 2013. Accepted on June 26, 2013.

voltage. Despite the fact that it has an almost flat frequency response up to about 50 MHz, the effect of it as well as the effect of the power grid that feeds the DUTs have been compensated by the VNA. In fact, we have fixed the calibration reference of the VNA after the coupler, on the power grid side.

Interestingly, we have found a limited number of devices characterized by a strong time variant behavior, namely, time variant loads. In addition, all the above time variant loads, except one (a Bluetooth headset charger), have exhibited two states of impedance with a rate of 100 Hz. As it will be explained in the following analysis, the limited number of time variant devices is due to the fact that most of the modern power supplies are designed in such a way to minimize the generation of unwanted harmonics on the input current waveform through the use of noise suppression capacitors or more complex EMI filters. The scarcity of time variant devices with a rate of 50 Hz is instead due to the deployment of full-wave rectifiers instead of inefficient half-wave rectifiers that have limited usage in modern power supplies.

In the next section, we will describe in detail the front-end block of the power supply unit. In particular, we analyze the power supply unit equipped with uncontrolled diode rectifiers.

A. Front-end of the Power Supply Unit

Basically, the front-end of most of the power supply units consists of an uncontrolled diode rectifier circuit and a “bulk” capacitor [17] that converts the input sinusoidal signal to a DC voltage. The process of continuously charging and discharging the “bulk” capacitor causes abrupt pulses of current when the instantaneous rectified voltage is higher than the DC voltage across the capacitor, which forwards biases the rectifier circuit [17]. Depending on the particular configuration of the rectifier circuit, the pulse of current appears twice or once during a mains period of 20 ms. In full-wave uncontrolled rectifiers that use a diode bridge, the pulse of current appears every half mains cycle when two of the four diodes of the bridge are forward biased. In half-wave uncontrolled rectifiers that use a single diode, the pulse of current appears once during the positive cycle of the mains signal, when the single diode is forward biased. Therefore, the relation between voltage and current is not linear. However, two states of the impedance can be

Submitted on February 2013. Revised on May 10, 2013 and on June 22, 2013. Accepted on June 26, 2013.

distinguished which allows us to model the load as having a periodically time variant impedance [9]. The impedance variation between states has periodicity of 10 or 20 ms depending on the aforementioned uncontrolled rectifier circuitry, respectively a rate of 100 Hz or 50 Hz.

The time variant behavior of some devices is simply caused by the uncontrolled rectifier of the front-end circuitry of the power supply unit and it is not amenable to DIAC, TRIAC or SCR diodes of the internal circuitry, as speculated in [9]. To substantiate this argument, we applied the following measurement procedure. We have identified two devices (a mobile phone charger and a compact fluorescent lamp (CFL)) inside which the electronic components just mentioned are present. As shown in Fig. 2, the impedance variations have been encountered at the peaks of the magnitude of the mains waveform, i.e., when the instantaneous voltage rectified by the full-wave uncontrolled diode rectifier is higher than the DC voltage across the internal "bulk" capacitor of the front-end circuitry of the power supply unit. In Fig. 2, we also report the mains waveform and the current pulses generated by the full-wave uncontrolled diode rectifier to highlight that the impedance variations have been encountered when the current pulses occur.

Thus, we have applied different AC voltages to the DUTs by a test network and we have characterized their behavior under different conditions. We have applied a very low voltage (such that the diodes of the uncontrolled rectifier circuit are not forward biased) and a higher voltage (such that the diodes of the uncontrolled rectifier circuit are forward biased but not sufficiently to switch ON the internal driver circuit of the device). In the first case, we have noted the total absence of a time variant behavior of the DUTs, while in the second case we have noticed a behavior identical to when the DUTs are supplied by the mains voltage. Therefore, we have concluded that the time variant behavior is simply due to the generation of current pulses by the front-end circuitry of the power supply unit. Indeed, the actual impedance value and the duration of each of the two distinct states of impedance are a function of the applied voltage and the overall load circuitry and condition.

Despite the fact that the front-end of the power supply unit exhibits a time variant impedance, the

Submitted on February 2013. Revised on May 10, 2013 and on June 22, 2013. Accepted on June 26, 2013.

presence of an EMI filter significantly reduces it, as we will discuss in the following section.

III. Effect of the EMI Filter

The measurement campaign has also shown that the noise suppression capacitors or, more precisely, the EMI filters attenuate the load impedance time variant behavior in the frequency range 2-30 MHz. In this respect, we have identified two mobile chargers. The first one has a strong time variant behavior as it is shown in Fig. 2. The second one, from a different manufacturer, has different time/frequency characteristics. In fact, it exhibits a time invariant behavior whose magnitude of the impedance is monotonically increasing up to 50 Ω within the frequency band 2-30 MHz, as it is shown in Fig. 3. The phase of the impedance has also a time invariant behavior, as it will be discussed in the following.

The internal circuitry of the two DUTs has been analyzed and it has been found that the rectifier circuit of both devices is a full-wave uncontrolled rectifier, but the second mobile phone charger is equipped with a noise suppression capacitor between the line and the neutral terminals on the input stage of the power supply unit. Thus, we searched for other devices whose magnitude of the impedance is time invariant and monotonically increasing. Electronic ballasts for halogen lamps and PC power supplies belong to this class of devices. It has been found that all of them deploy an EMI filter or a noise suppression capacitor between the line and the neutral terminals. Although there exist several different types of EMI filters, they all use at least one line-to-line capacitor, also known as X-cap, whose goal is to suppress differential mode currents that flow along the line (hot) conductor and return through the neutral one [17]. More details are given in Appendix A. The magnitude of the impedance of the line-to-line capacitor is relatively small compared to the impedance of the device without the noise suppression capacitor within the frequency band 2-30 MHz. Thus, the X-cap imposes a low impedance value and it reduces any significant impedance variation.

To experimentally prove that the EMI filter reduces the device impedance time variations, we have selected a PC power supply and physically removed all the electronic components composing the EMI filter. Then, we have performed a new measurement. As expected, we have found that with this

Submitted on February 2013. Revised on May 10, 2013 and on June 22, 2013. Accepted on June 26, 2013.

configuration the time variant behavior is exhibited. In Fig. 4, we show the magnitude of the impedance of the PC power supply under test for different time instants within a period T of the mains waveform, with and without the EMI filter circuitry. We denote with T_{ON} and T_{OFF} the time intervals where the diodes of the uncontrolled rectifier circuit are, or are not, forward biased respectively. The figure shows that the magnitude of the impedance of the device without the EMI filter is higher than the impedance of the device with the EMI filter and variations are exhibited only without the EMI filter. Furthermore, in Fig. 5-(a) we show that the impedance of the PC power supply under test is equal to the impedance of the X-cap in the frequency range 2-30 MHz.

Now, the low values and the monotonically increasing profile of the magnitude of the impedance are due to the parasitic inductance of the lead wires of the X-cap (as confirmed with measurements). The lumped circuit model that yields considerable insight into the non-ideal behavior of a real capacitor is the series combination of an ideal capacitance C, a certain inductance due to the component attachment leads L_l and an equivalent series resistance (ESR) R_{ESR} [17]. As shown in Fig. 5-(b), at low frequencies, the impedance of the capacitor is dominant and the magnitude of the impedance of the real capacitor is $|Z(f)| \approx 1/(2\pi fC)$ which decreases with frequency. As frequency increases, the effect of the parasitic inductance becomes not negligible, and its impedance reads $|Z(f)| \approx 2\pi f L_l$. At the self-resonant frequency of the capacitor $f_0 = 1/2\pi\sqrt{L_l C}$ [17], the impedances of the ideal capacitor and of the parasitic inductance are the same and equal to the ESR resistance [17]. In Fig. 5-(b), we can notice that the self-resonant frequency of the 0.33 μF noise suppression capacitor is at about 700 kHz. After this frequency, the impedance of the real capacitor is dominated by the parasitic inductor and it increases linearly with frequency. As a consequence, the phase of the impedance assumes a constant and time invariant value equal to $+\pi/2$.

It should be noted that the above considerations are valid for frequencies above 2 MHz, since the self-resonance frequency of the common noise suppression capacitors is always smaller than 2 MHz.

Submitted on February 2013. Revised on May 10, 2013 and on June 22, 2013. Accepted on June 26, 2013.

IV. On the Power Cord Effect

So far, we have considered devices without a power cord. The measurement campaign has shown that the power cord has also a significant effect on the resulting impedance of the devices. Most of the devices that we can find in a house or office have a power cord with length that ranges from tens of centimeters, e.g., for a laptop adapter, to meters, e.g., for a vacuum cleaner.

As it will be shown in the following, the magnitude of the impedance of these devices exhibits a series of damping peaks and nulls at regular intervals within the 2-30 MHz considered frequency band. At the frequencies where the peaks occur, the devices act as parallel resonant circuits and their behavior swaps from inductive to capacitive. Conversely, at the impedance nulls the devices behave as series resonant circuits, moving from a capacitive to an inductive behavior. At the parallel and series resonant frequencies, the phase of the impedance is always zero and the devices act respectively as a high or low purely resistive load.

We can explain such a behavior using transmission line (TL) theory concepts. The power cord acts as a transmission line of length L characterized by its characteristic impedance $Z_c(f)$ and its propagation constant $\gamma(f)$. The propagation constant is defined as $\gamma(f) = \alpha(f) + j\beta(f)$, where $\alpha(f)$ and $\beta(f)$ are the attenuation and phase constants, respectively, and j is the imaginary unit. In Fig. 6, we show the profiles of the aforementioned constitutive parameters of a typical 3-wires power cable (3x1.5 mm^2 *H05VV-F* flexible cable, insulated and outer sheathed in PVC), obtained via measurements.

The resonant behavior is due to the impedance mismatch between the line characteristic impedance and the impedance of the load at the end of the power cord. The decreasing profile of the amplitude of the peaks with frequency is instead amenable to the resistive losses of the cable. The number of peaks and nulls within the considered frequency band is variable and it depends on the length of the cable and on its constitutive parameters.

In the following, we show that it is possible to predict the impedance of the devices equipped with a

Submitted on February 2013. Revised on May 10, 2013 and on June 22, 2013. Accepted on June 26, 2013.

power cord. We assume such devices composed by a low losses transmission line terminated in a purely resistive load R_L. Therefore, the device impedance reads

$$Z(f) = Z_c(f)\frac{R_L + Z_c(f)\tanh(\gamma(f)L)}{Z_c(f) + R_L\tanh(\gamma(f)L)}. \quad (1)$$

The value of the purely resistive load that best fits the impedance profile of the measured devices is obviously a function of the constitutive parameters of the power cord and of its length. In Appendix B, we provide more details and we propose an analytic expression for R_L that allows us to fit the measurements. An excellent agreement is found between the model in (1) and the measured impedances.

In detail, in Fig. 7 we show the comparison of the magnitude and the phase of the impedance of two devices equipped with a power cord whose behavior at low frequencies (before the first resonant frequency) is inductive, i.e., an hairdryer (Figs. 7-(a1),(b1)) and a switched ON vacuum cleaner (Figs. 7-(a2),(b2)). In Fig. 8, we compare the results of two different devices equipped with a power cord whose behavior at low frequencies (before the first resonant frequency) is capacitive, i.e., a desk lamp (Figs. 8-(a1),(b1)) and the same vacuum cleaner of Fig. 7, but switched OFF (Figs. 8-(a2),(b2)).

This distinction will be discussed in the following section. Furthermore, it should be noted that herein we have considered time invariant loads but the effect of the power cord is essentially the same in LPTV loads.

V. Classification of the Measured Devices

Overall, the devices have a behavior that belongs to four classes. In the following, such classes are described and representative impedance profiles are shown. Firstly, we can divide the devices between those characterized by a time variant or a time invariant impedance. Focusing on the time invariant loads, we propose three classes. A first macro classification can be made according to the profile of the magnitude of the impedance. If it is monotonically increasing, as for the devices without a power cord and equipped with an X-cap between the two feeding conductors, the load can be included in Class A. Class A comprises the devices listed in Table I. In Fig. 9, we show the magnitude and phase of the impedance of three

Submitted on February 2013. Revised on May 10, 2013 and on June 22, 2013. Accepted on June 26, 2013.

representative devices. We highlight the fact that these devices belong to this macro class regardless of what their operating state is (switched ON or OFF).

If the magnitude of the impedance exhibits damping peaks and nulls within the considered 2-30 MHz band the load can be included in Class B. Devices with a power cord and time invariant behavior, e.g., those that have an EMI filter, fall in this class. The devices of Class B are further classified into two subclasses according to their behavior at low frequencies (before the first resonant frequency), i.e., if it is inductive (Class B-1) or capacitive (Class B-2). This is equivalent to discriminate whether the profile of the impedance exhibits a peak or a null at the first resonant frequency (in the band 2-30 MHz). In Table II and Table III, we list the aforementioned devices and, in Fig. 10 and Fig. 11, we show the magnitude and phase of the impedance of three representative devices. Some devices may be included in both subclasses, according to their operating state (switched ON or OFF). These devices essentially consist of an electrical motor. The devices belonging to Class B-1, regardless of what their operating state is (switched ON or OFF), are characterized by a low impedance at the end of the power cord. These devices are certainly equipped with an X-cap between the two feeding conductors that imposes a low impedance value as discussed in Section III. From these considerations, some of the devices belonging to the Class A, i.e., the halogen lamps with electronic ballasts and the PC power supplies, can be included into this subclass when they are supplied using a power cord whose length is not negligible.

Conversely, the devices belonging to Class B-2, regardless of what their operating state is, are characterized by a high impedance at the end of the power cord. These devices are equipped with a particular power supply unit whose input stage is a power transformer followed by an EMI filter that induces a time invariant behavior.

In Tables II and III, we have included the length of the power cord. We remark that the number of peaks and nulls within the considered frequency band is variable and it depends on the constitutive parameters of the cable and on its length. In particular, as shown by (5) in the Appendix B, the longer the cable, the larger

Submitted on February 2013. Revised on May 10, 2013 and on June 22, 2013. Accepted on June 26, 2013.

the number of peaks and nulls is.

Given the rarity of devices characterized by strong time variant behavior, we propose a single macro class for them, i.e., Class C. In Table IV, we list the measured devices belonging to this class and we report the time variation rate (TV rate). In Fig. 12, we show the magnitude and the phase of the two impedance states for one representative device of Class C, i.e., a compact fluorescent lamp. It should also be noted that if the time-variant device is equipped with a power cord with non-negligible length, considerations similar to those made for Class B-1 and B-2 can be made. That is, the profile of each of the two impedance states will be similar to that in Class B-1 or Class B-2.

It should be noted that the classification based on type of device does not always work since what determines the impedance profile is the input stage of the power supply block, i.e.,, the classification is behavioral and the behavior depends on the circuitry. For instance, a distinction between time variant and time invariant loads by type of device is not always possible since similar devices from different manufactures may have different characteristics, e.g., they may be equipped with different power supplies or circuitry for the noise and the EMI suppression. A prediction about what class a device belongs to, and consequently, what impedance profile it has, can be done by looking at the input stage of the power supply block. For instance, devices with an X-cap and no power cord go in Class A, devices with power cord fall in Class B1/B2, devices with power supply unit without EMI filter go in Class C.

VI. CONCLUSIONS

In this paper we have dealt with the analysis of the load impedances that are present in home power grids. The analysis is motivated by the fact that such loads affect the PLC channel and modeling them is important in bottom-up channel simulators. We have performed a measurement campaign on a representative and sufficiently general set of devices that can be found in a typical house or office, i.e., a number of home appliances, office equipment and lighting system components. We have investigated the frequency behavior of such devices in terms of the voltage-to-current relation between the two feeding

Submitted on February 2013. Revised on May 10, 2013 and on June 22, 2013. Accepted on June 26, 2013.

conductors, i.e., the line and the neutral wires, in the frequency range 2-30 MHz. A limited number of devices that exhibit a periodically time variant impedance with repetition frequency that is an integer multiple of the mains frequency, has been found. We have shown that what causes the impedance time variations is the front-end circuitry of the power supply unit. In fact, the generation of current pulses when the diodes of the uncontrolled rectifier circuits are forward biased, leads to a nonlinear relation between voltage and current. Nevertheless, a two states linear relation can be defined. The actual impedance value and the duration of each of the two distinct states are a function of the load circuitry and condition. However, most of the loads deploy an EMI filter or noise suppression capacitor between the line and the neutral terminals which significantly reduces the impedance time variations. We have experimentally proven the above considerations. The effect on the impedance of the power cord used to connect a certain device into the home power grid has also been considered.

From the experimental results we have proposed a behavioral classification of the measured devices according to their time/frequency characteristics and we have reported representative impedance profiles and a modeling approach. Based on the results, for networks where most of the loads are time invariant, the PLC channel response is expected to be practically time invariant, as confirmed also by the channel measurements in Italian home networks [19]. A more pronounced time variant behavior is expected in channels belonging to the lighting circuit if, for instance, several compact fluorescent lamps without an EMI filter are used.

APPENDIX A – EMI FILTERS

An electromagnetic interference (EMI) filter is a low-pass passive filter properly designed to suppress the electromagnetic and the noise emissions generated by the electronic devices and conducted through the line, neutral and ground wires to the power grid. For the conducted emissions, the electromagnetic norms EN 55022/CISPR 22 regulate the frequency range from 150 kHz to 30 MHz [17]. Two distinct components can be distinguished, i.e., the differential mode (DM) and the common mode (CM) emissions. The DM

Submitted on February 2013. Revised on May 10, 2013 and on June 22, 2013. Accepted on June 26, 2013.

ones are those that flow from the line (hot) conductor to the neutral wire, while the CM emissions flow in the same direction on the line and the neutral conductors and return through the ground. As depicted in Fig. 13, the EMI filter is essentially composed of a capacitive and an inductive part. The capacitive part consists of two kind of capacitors which provide bypass paths to the high frequency currents. C_x denotes the line-to-line capacitor, also known as X-cap [17], installed between the line and neutral terminals. At high frequencies, the C_x capacitor acts as a short circuit path for the differential mode currents and it can assume high capacitance values, i.e., typically tens or hundreds nF [17].

Therefore, at the mains frequency of 50 Hz, the effect of the X-cap is negligible, so that it does not interfere with the feeding power signal. C_y denotes the two line-to-ground capacitors, or Y-caps [17], between the line and the ground terminals and between the neutral and the ground wires. The two capacitors are used to suppress common mode currents. Typical values are few nF [17], due to safety reasons. In fact, low impedance paths between the line (or the neutral) wires and the ground conductor have to be avoided at frequency 50 Hz. The inductive part is essentially composed of a common mode choke, represented in Fig. 13 by the two coupled inductors (L_1, L_2 and the mutual inductance M) that acts as a transparent device at frequency 50 Hz for the mains signal and blocks the common mode currents at high frequencies.

APPENDIX B – DERIVATION OF AN ANALYTIC EXPRESSION OF R_L IN (1)

The input impedance of a low losses transmission line terminated in a purely resistive load R_L reads as (1). The parallel and series resonant frequencies discussed in Section IV are those at which the input impedance is purely real. Now, we focus on the analytic derivation of such frequencies. We proceed as follows. Via measurements, we have found that the dielectric constant $\varepsilon(f)$ in several common power cords can be expressed as

Submitted on February 2013. Revised on May 10, 2013 and on June 22, 2013. Accepted on June 26, 2013.

$$\varepsilon(f) = \varepsilon_0 \left[\frac{K}{f} + \varepsilon_\infty \right], \tag{2}$$

where ε_0 is the vacuum dielectric constant, K is a weighting factor and ε_∞ is the asymptotic relative dielectric constant. Via measurements we can obtain the per-unit-length (p.u.l.) constitutive parameters of some common 2-wires and 3-wires power cables, i.e., the p.u.l. resistance $r(f)$ (Ω/m), conductance g (S/m), capacitance $c(f)$ (F/m) and inductance l (H/m). The p.u.l. resistance increases at a rate proportional to $\sqrt{f}$ due to the skin effect [17], while the p.u.l. capacitance decreases as the dielectric constant. Thus, under the assumption of low losses transmission line [17], we can calculate the characteristic impedance and the propagation constant as

$$Z_c(f) \approx \sqrt{\frac{l}{c(f)}}, \tag{3}$$

$$\gamma(f) \approx \frac{r(f)}{2Z_c(f)} + j2\pi f\sqrt{lc(f)}. \tag{4}$$

Without any loss of generality, we also make the assumption that the p.u.l. resistance does not affect the phase constant. According to [20], if the medium that surrounds the conductors is homogeneous and is characterized by a magnetic permeability equal to the vacuum permeability μ_0 and has dielectric constant $\varepsilon(f)$, the p.u.l. inductance and the dielectric constant are related as $lc(f) = \mu_0\varepsilon(f)$. Therefore, from (4), $\beta(f) = 2\pi f\sqrt{lc(f)} = 2\pi f\sqrt{\mu_0\varepsilon(f)}$. As a consequence, the frequencies at which the input impedance is purely real read

$$f_0^{(m)} = \frac{K + \sqrt{K^2 + 4\varepsilon_\infty \left(\frac{m\nu_0}{2L}\right)^2}}{2\varepsilon_\infty}, \tag{5}$$

where $\nu_0 = 1/\sqrt{\mu_0\varepsilon_0}$ is the vacuum light speed, and $m = 0, 1, \ldots$ so that $tan(\beta(f)L) = 0$, while $m = 1/2, 3/2, \ldots$ so that $tan(\beta(f)L) \to \infty$. The first resonant frequency greater than 0 is $\hat{f}_0 = f_0^{(1/2)}$.

Given $\hat{f}_0$ and the measured impedance value of the DUT at that frequency, namely $\hat{Z}$, the purely resistive load R_L that allows an excellent fit with the measured impedances is obtainable from (1) as

Submitted on February 2013. Revised on May 10, 2013 and on June 22, 2013. Accepted on June 26, 2013.

$$R_L = Z_c(\hat{f}_0)\frac{\hat{Z}\tanh(\alpha(\hat{f}_0)L) \quad Z_c(\hat{f}_0)}{Z_c(\hat{f}_0)\tanh(\alpha(\hat{f}_0)L) \quad \hat{Z}}. \tag{6}$$

The desired input impedance $\hat{Z}$ at $\hat{f}_0$ can assume values in prefixed ranges to obtain real positive values of R_L, i.e., a peak at $\hat{f}_0$ for $\hat{Z} >> Z_c(\hat{f}_0) \wedge \hat{Z} < Z_c(\hat{f}_0)/\tanh(\alpha(\hat{f}_0)L)$, a null at $\hat{f}_0$ for $\hat{Z} > Z_c(\hat{f}_0)\tanh(\alpha(\hat{f}_0)L) \wedge \hat{Z} << Z_c(\hat{f}_0)$.

All of the measured devices satisfy this constraint. From (6), if the impedance of the device exhibits a peak at $\hat{f}_0$, the value of the purely resistive load R_L of the model will be low. Conversely, if the impedance exhibits a null, R_L will be high.

REFERENCES

[1] H. C. Ferreira, L. Lampe, J. Newbury, and T. G. Swart, *Power Line Communications: Theory and Applications for Narrowband and Broadband Communications over Power Lines*. NY: Wiley & Sons, 2010.

[2] H. Philipps, "Modeling of Power Line Communication Channels," in *Proc. IEEE Int. Symp. on Power Line Commun. and Its App. (ISPLC)*, Mar. 1999, pp. 14-21.

[3] F.J. Cañete, L. Díez, J.A. Cortés, and J.T. Entrambasaguas, "Broadband Modeling of Indoor Power-Line Channels", *IEEE Trans. on Consumer Electronics*, vol. 48, no. 1, pp. 175-183, Feb. 2002.

[4] M. Zimmermann and K. Dostert, "A Multipath Model for the Powerline Channel," *IEEE Trans. on Communications*, pp. 553-559, Apr 2002.

[5] A. Cataliotti, V. Cosentino, D. Di Cara, G. Tine, "Oil-Filled MV/LV Power-Transformer Behavior in Narrow-Band Power-Line Communication Systems," *IEEE Trans. on Instrumentation and Measurement*, vol. 61, no. 10, pp. 2642-2652, Oct. 2012.

[6] S. Barmada, A. Musolino, M. Raugi, "Upper and Lower Bounds for Frequency Response of PLC Channels in Presence of Load Variations," in *Proc. IEEE Int. Symp. on Power Line Commun. and*

Submitted on February 2013. Revised on May 10, 2013 and on June 22, 2013. Accepted on June 26, 2013.

Its App. (ISPLC), Mar. 2006, pp 12-15.

[7] J. Anatory, N. Theethayi, R. Thottappillil, M. M. Kissaka, and N. H. Mvungi, "The Influence of Load Impedance, Line Length, and Branches on Underground Cable Power-Line Communications (PLC) Systems," *IEEE Trans. on Power Delivery*, vol. 23, no. 1, pp. 180-187, Jan. 2008.

[8] D. Hirata, N. Kuwabara, Y. Akiyama, and H. Yamane, "Influence of Appliance State on Transmission Characteristics of Indoor AC Mains Lines in Frequency Range Used Power Line Communication," in *Proc. Int. Symp. on Electromagnetic Compatibility (EMC)*, Aug. 2005, vol.3, pp. 715-720.

[9] F. J. Cañete, J. A. Cortés, L. Díez, and J. T. Entrambasaguas, "Analysis of the Cyclic Short-Term Variation of Indoor Power Line Channels," *IEEE J. on Sel. Areas in Commun.*, vol. 24, no. 7, pp. 1327-1338, Jul. 2006.

[10] T. Esmailian, F. R. Kschischang, and P. Glenn Gulak, "In-Building Power Lines as High-Speed Communication Channels: Channel Characterization and a Test Channel Ensemble," *Intern. J. of Commun. Syst.*, vol. 16, no. 5, pp. 381-400, Jun. 2003.

[11] A. M. Tonello, and F. Versolatto, "Bottom-Up Statistical PLC Channel Modeling-Part I: Random Topology Model and Efficient Transfer Function Computation," *IEEE Trans. on Power Delivery*, vol. 26, no. 2, pp. 891-898, April 2011.

[12] A. M. Tonello, and F. Versolatto, "Bottom-Up Statistical PLC Channel Modeling-Part II: Inferring the Statistics," *IEEE Trans. on Power Delivery*, vol. 25, no. 4, pp. 2356-2363, Oct. 2010.

[13] M. Zimmermann and K. Dostert, "Analysis and Modeling of Impulsive Noise in Broadband Powerline Communications," *IEEE Trans. on Electromagnetic Compatibility*, vol. 44, pp. 249–258, Feb. 2002.

[14] J. A. Cortés, L. Diez, F. J. Cañete, and J. J. Sanchez-Martinez, "Analysis of the Indoor Broadband Power-Line Noise Scenario," *IEEE Trans. on Electromagnetic Compatibility*, vol. 52, pp. 849–858,

Submitted on February 2013. Revised on May 10, 2013 and on June 22, 2013. Accepted on June 26, 2013.

Nov. 2010.

[15] I. Yokoshima, "RF Impedance Measurements by Voltage-current Detection," *IEEE Trans. on Instrumentation and Measurement*, vol. 42, no. 2, pp. 524-527, Apr 1993.

[16] L. Angrisani, A. Baccigalupi, A. Pietrosanto, "A Digital Signal-processing Instrument for Impedance Measurement," *IEEE Trans. on Instrumentation and Measurement*, vol. 45, no. 6, pp. 930-934, Dec 1996.

[17] R. P. Clayton, *Introduction to Electromagnetic Compatibility*, 2nd Edition. Wiley-Interscience, 2005.

[18] D. Zhang, D.Y. Chen, M. J. Nave, D. Sable, "Measurement of Noise Source Impedance of Off-line Converters," *IEEE Trans. on Power Electronics*, vol. 15, no. 5, pp. 820-825, Sep 2000.

[19] F. Versolatto, A.M. Tonello, "PLC Channel Characterization up to 300 MHz: Frequency Response and Access Impedance," *in Proc. of IEEE Global Telecommunications Conference (GLOBECOM) 2012*, Anaheim, California, USA, December 3-7, 2012.

[20] R. P. Clayton, *Analysis of Multiconductor Transmission Lines*, 2nd Edition. Wiley-IEEE Press, 2007.

Submitted on February 2013. Revised on May 10, 2013 and on June 22, 2013. Accepted on June 26, 2013.

TABLES

TABLE I
CLASS A - TIME INVARIANT DEVICES WITHOUT POWER CORD

Device Under Test	Operating state
PC power supply (Fig. 5-(a))	ON/OFF
Halogen lamp with electronic ballast	ON/OFF
Mobile phone charger (Fig. 3)	ON/OFF

TABLE II
CLASS B-1 - TIME INVARIANT DEVICES WITH POWER CORD (INDUCTIVE)

Device Under Test	Operating state	Cable length L [m]
Vacuum cleaner	ON	10
Drill	ON	1
Vending coffee machine	ON	3
Refrigerator	ON	3
Hairdryer	ON/OFF	1.80
Microwave oven	ON/OFF	2
DVD Player	ON/OFF	2
Cooking mixer	ON/OFF	1.5

TABLE III
CLASS B-2 - TIME INVARIANT DEVICES WITH POWER CORD (CAPACITIVE)

Device Under Test	Operating state	Cable length L [m]
Vacuum cleaner	OFF	10
Drill	OFF	1
Vending coffee machine	OFF	3
Refrigerator	OFF	3
Desk lamp	ON/OFF	1.80
CD Player	ON/OFF	2
Electrical steam cooker	ON/OFF	1
Audio amplifier	ON/OFF	1

TABLE IV
CLASS C - TIME VARIANT DEVICES WITHOUT POWER CORD

Device Under Test	TV Rate [Hz]
Compact fluorescent lamp	100
Mobile phone charger (Fig. 2)	100
Bluetooth headset charger	50

Submitted on February 2013. Revised on May 10, 2013 and on June 22, 2013. Accepted on June 26, 2013.

FIGURES

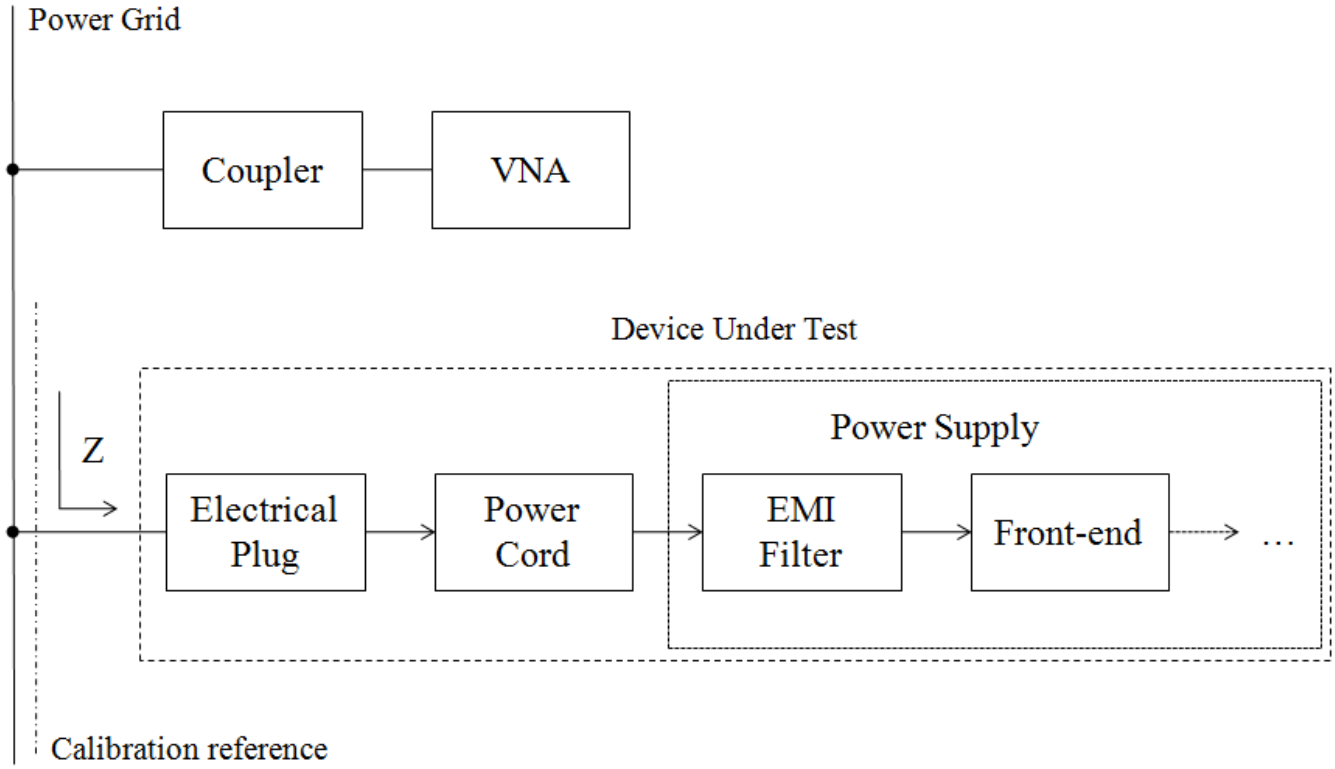

Fig. 1. Schematic of the load impedance measurement setup and the block diagram of the input stage of typical electrical devices.

Submitted on February 2013. Revised on May 10, 2013 and on June 22, 2013. Accepted on June 26, 2013.

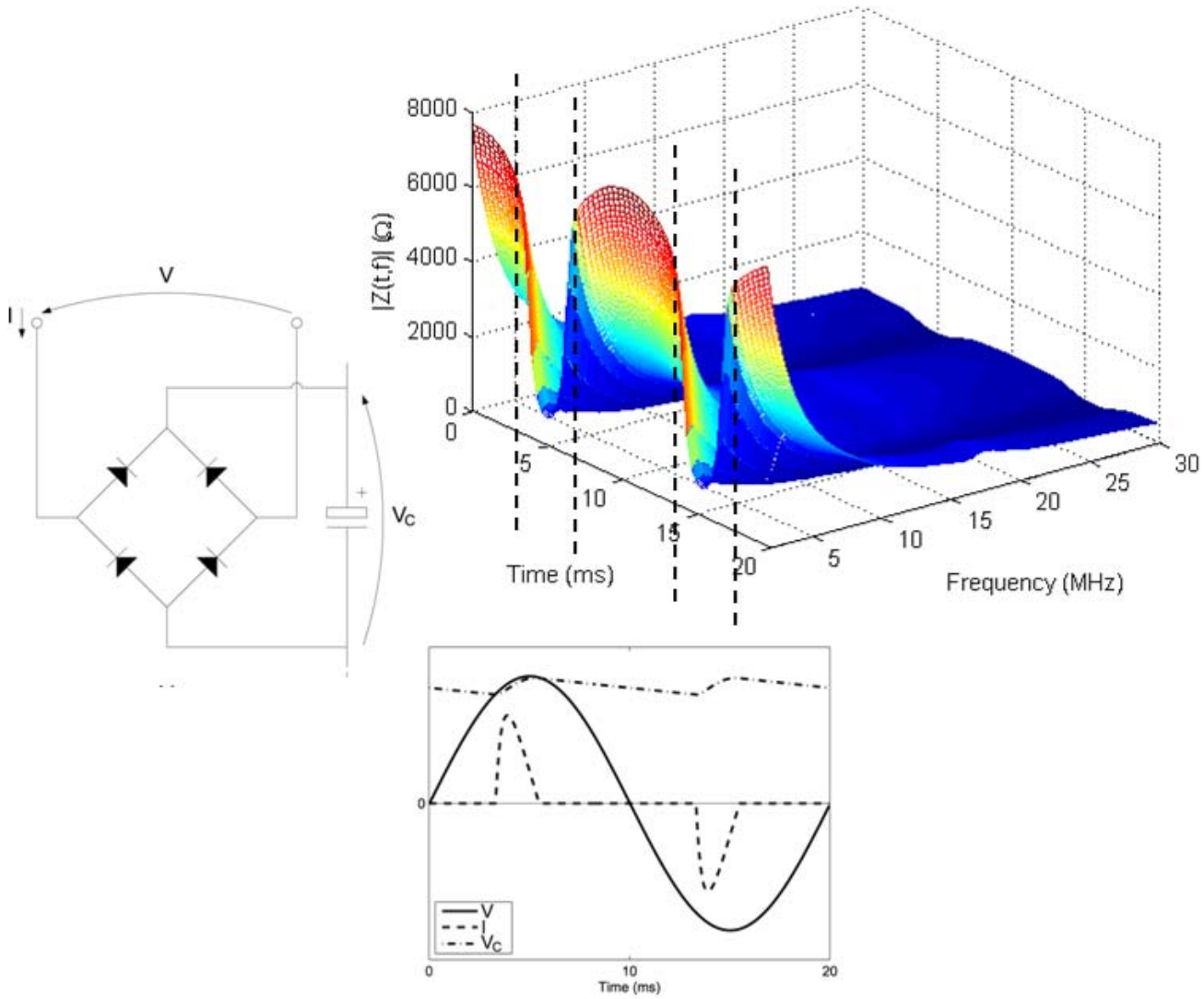

Fig. 2. Magnitude of the impedance of a highly time variant mobile phone charger under test, during a time span equal to the mains period. The time instant 0 ms corresponds to the zero-crossing of the mains waveform (rising edge). The mains waveform and the current pulses generated by the full-wave uncontrolled diode rectifier of the front-end of the power supply unit are reported to highlight that the impedance variations have been encountered at the peaks of the magnitude of the mains waveform, i.e., when the instantaneous rectified voltage is higher than the DC voltage across the internal "bulk" capacitor.

Submitted on February 2013. Revised on May 10, 2013 and on June 22, 2013. Accepted on June 26, 2013.

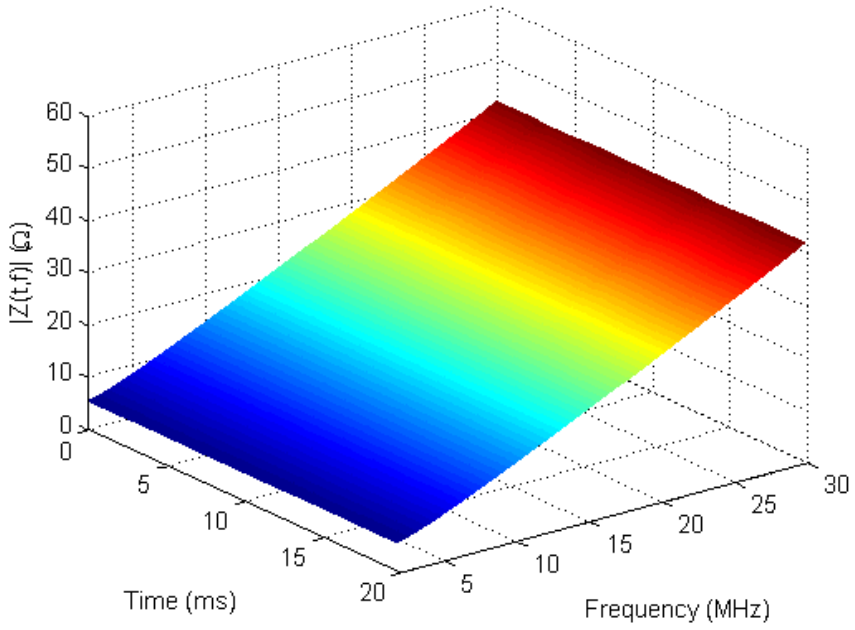

Fig. 3. Magnitude of the impedance of a time invariant mobile phone charger, during a time span equal to the mains period.

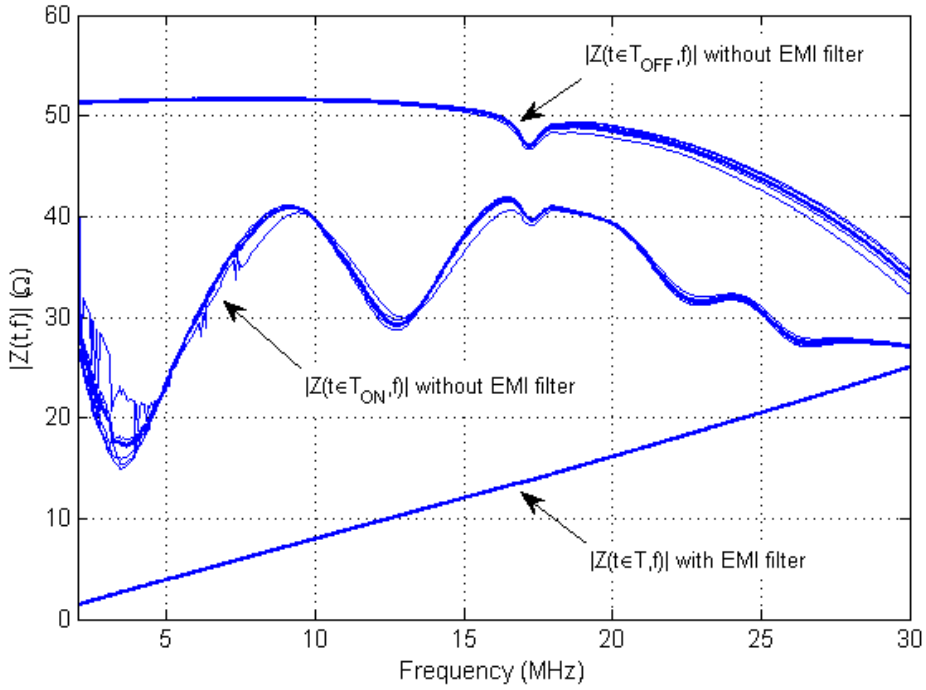

Fig. 4. Magnitude of the impedance of the PC power supply under test for different time instants within a period of the mains signal, with and without EMI filter circuitry. T is the period of the mains waveform, T_{ON} and T_{OFF} are the time intervals when the diodes of the uncontrolled rectifier circuit are respectively forward biased or they are not.

Submitted on February 2013. Revised on May 10, 2013 and on June 22, 2013. Accepted on June 26, 2013.

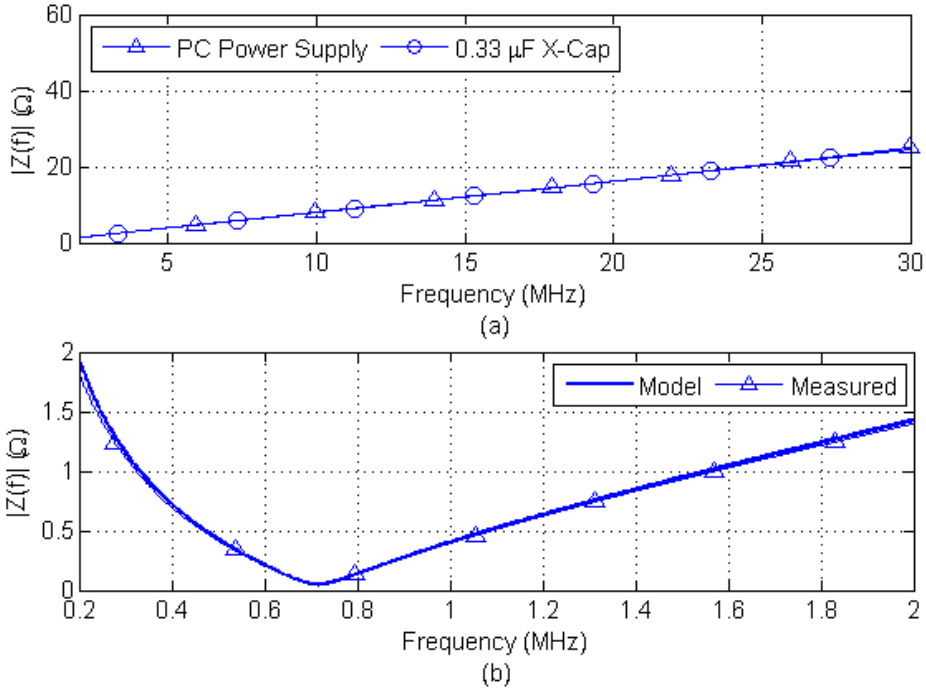

Fig. 5. (a) Magnitude of the impedance of the PC power supply under test and of the X-cap of its EMI filter and (b) comparison between the magnitude of the impedance of the X-cap and of the lumped circuit model, within an extended frequency range (200 kHz-2 MHz).

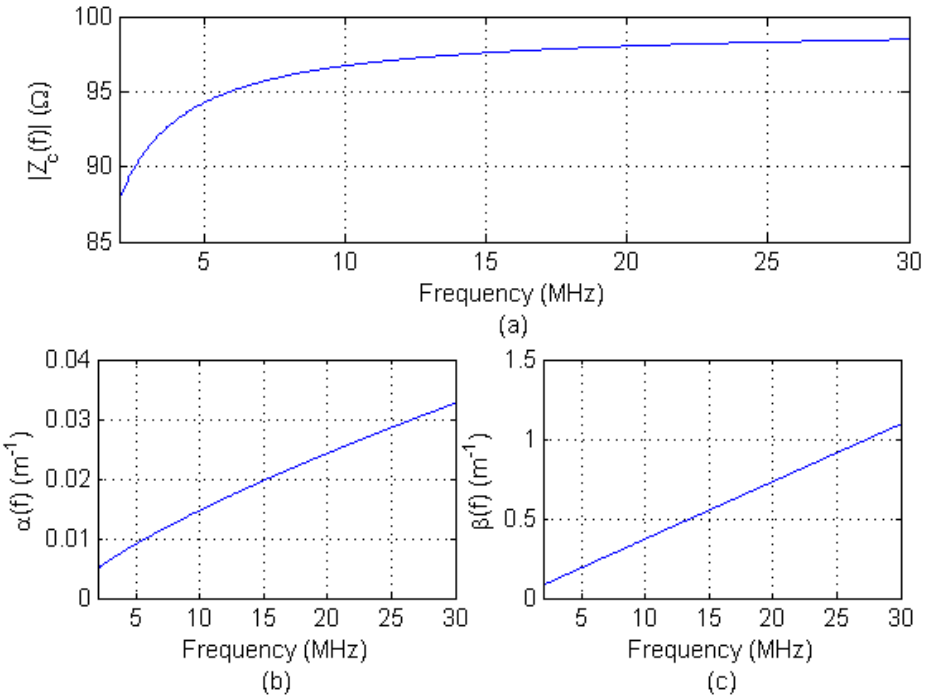

Fig. 6. (a) Profile of the characteristic impedance $Z_c(f)$, (b) of the attenuation constant $\alpha(f)$, (c) of the phase constant $\beta(f)$, of a typical 3-wires power cable (3x1.5 mm2 *H05VV-F* flexible cable, insulated and outer sheathed in PVC).

Submitted on February 2013. Revised on May 10, 2013 and on June 22, 2013. Accepted on June 26, 2013.

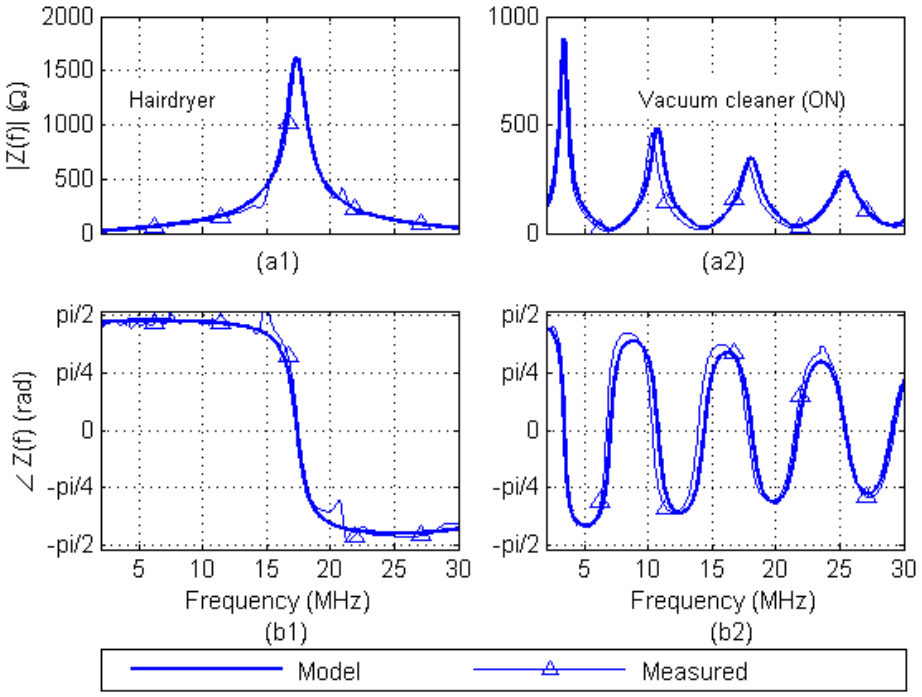

Fig. 7. (a1)-(a2) Magnitude and (b1)-(b2) phase of measured and modeled impedance of two devices under test equipped with a power cord whose behavior at low frequencies (before the first resonant frequency) is inductive.

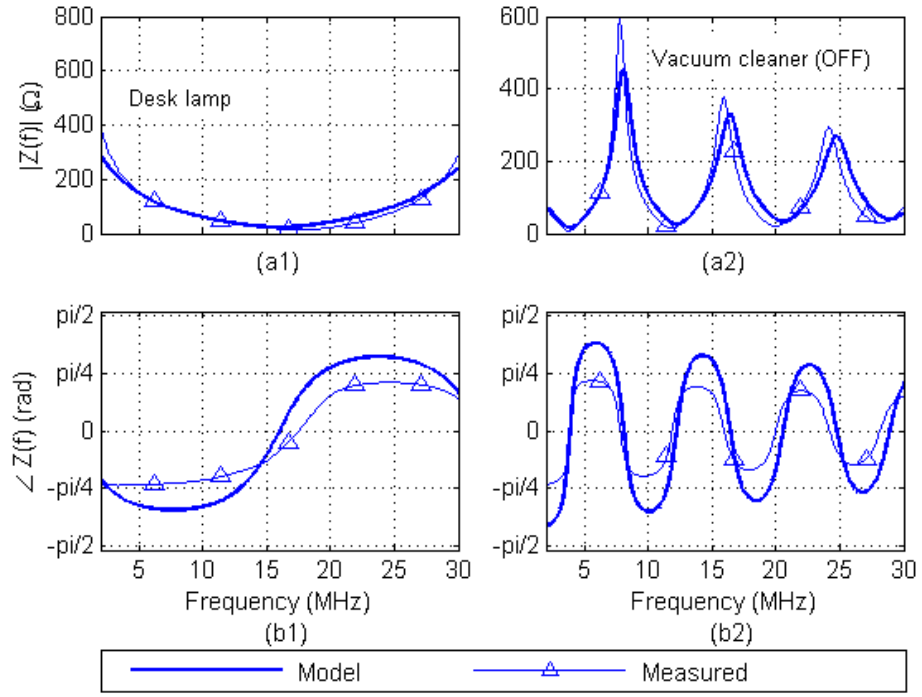

Fig. 8. (a1)-(a2) Magnitude and (b1)-(b2) phase of measured and modeled impedance of two devices under test equipped with a power cord whose behavior at low frequencies (before the first resonant frequency) is capacitive.

Submitted on February 2013. Revised on May 10, 2013 and on June 22, 2013. Accepted on June 26, 2013.

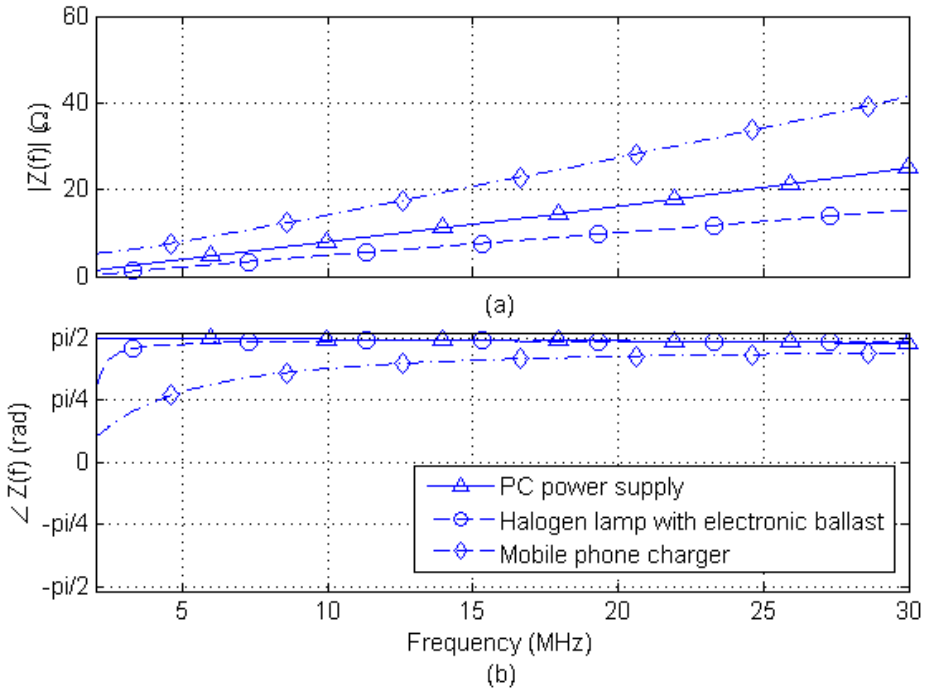

Fig. 9. (a) Magnitude and (b) phase of the impedance of three representative devices of Class A.

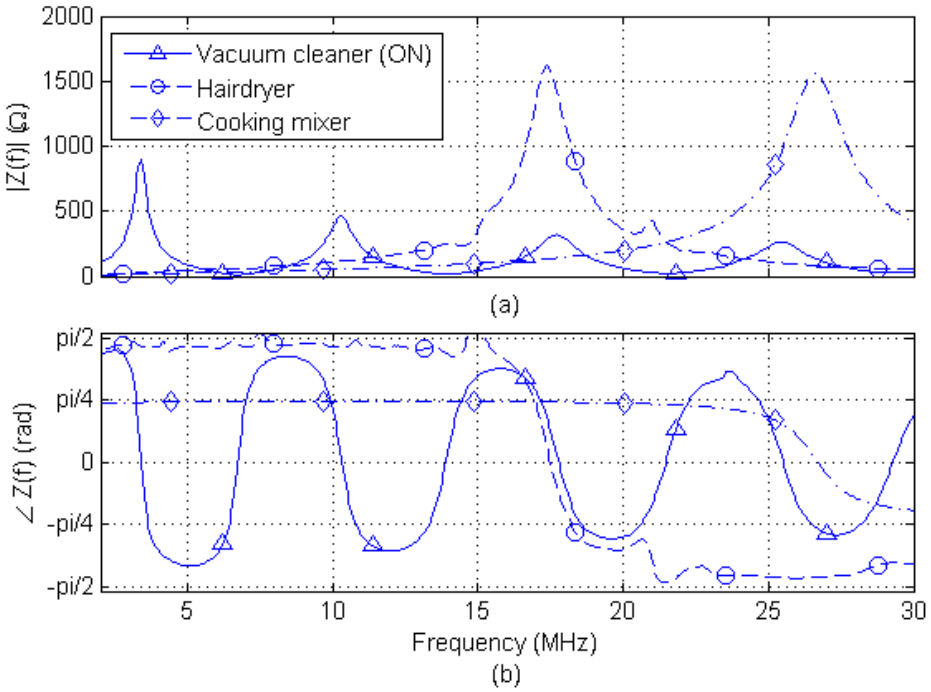

Fig. 10. (a) Magnitude and (b) phase of the impedance of three representative devices of Class B-1.

Submitted on February 2013. Revised on May 10, 2013 and on June 22, 2013. Accepted on June 26, 2013.

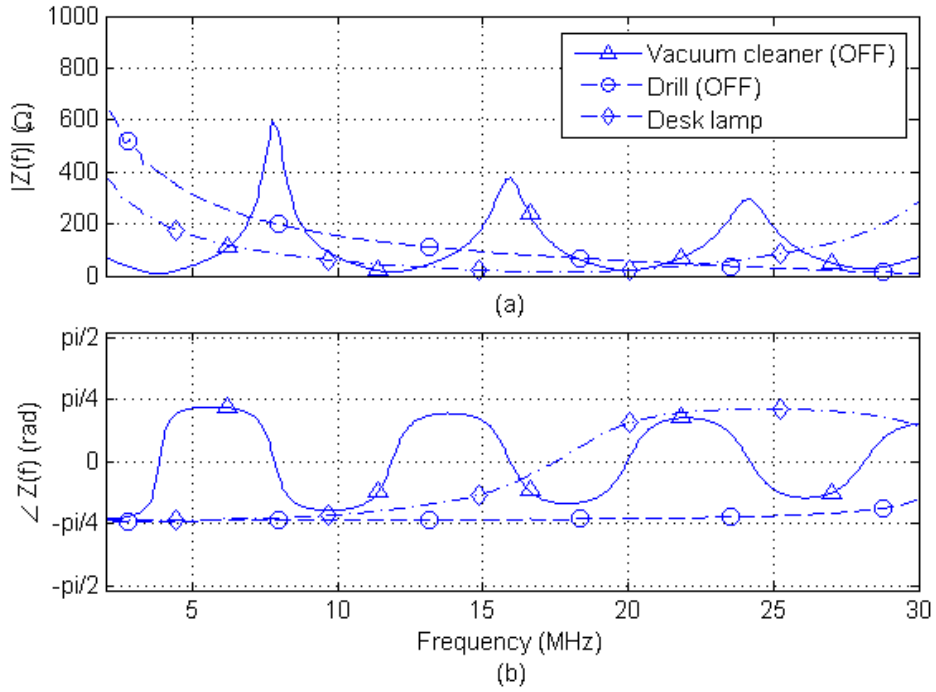

Fig. 11. (a) Magnitude and (b) phase of the impedance of three representative devices of Class B-2.

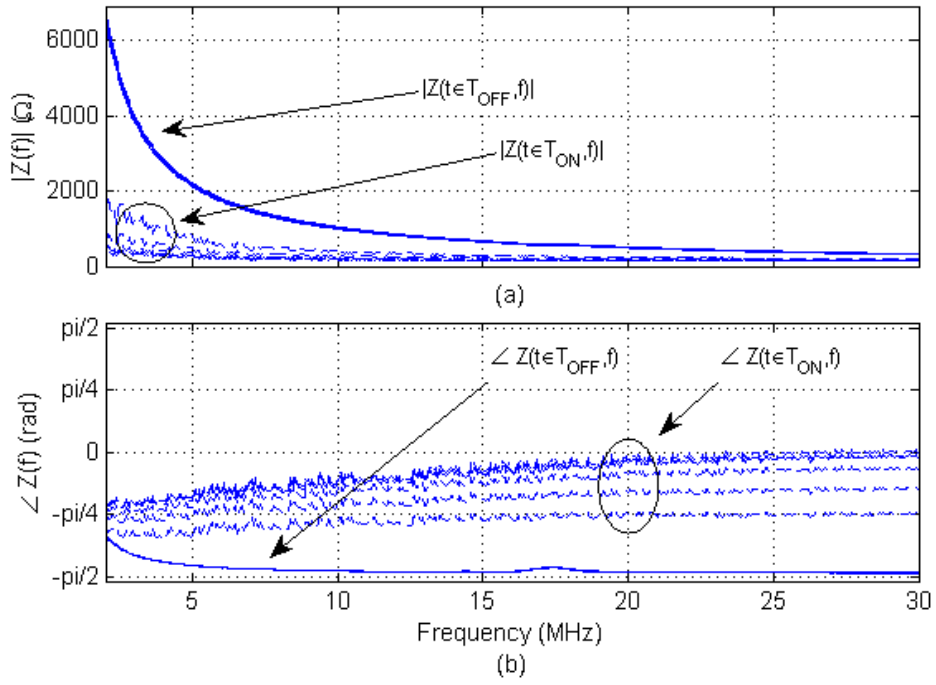

Fig. 12. (a) Magnitude and (b) phase of the impedance of the compact fluorescent lamp belonging to Class C, shown every 2 ms.

Submitted on February 2013. Revised on May 10, 2013 and on June 22, 2013. Accepted on June 26, 2013.

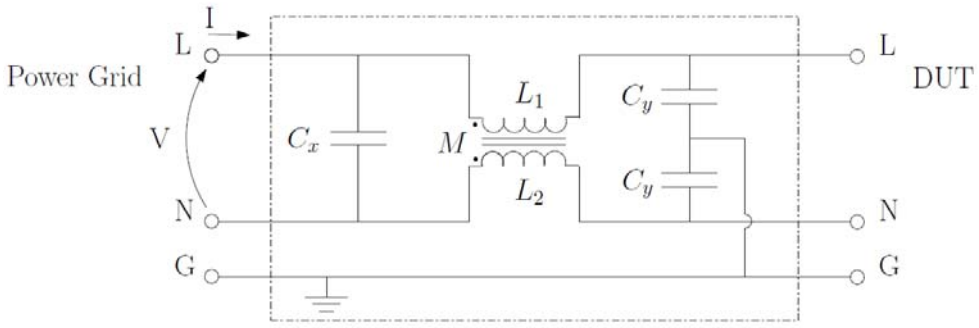

Fig. 13. Circuit schematic of a typical EMI filter.